Zinc-dependent activation of the Pho8 alkaline phosphatase in *Schizosaccharomyces pombe*

Received for publication, January 2, 2019, and in revised form, June 20, 2019 Published, Papers in Press, June 25, 2019, DOI 10.1074/jbc.RA119.007371

Ya-Mei Hu[‡], Derek M. Boehm[§], Hak Chung[¶], Stevin Wilson[§], and Amanda J. Bird[‡§‖1]

From the Departments of [‡]Human Nutrition and [§]Molecular Genetics, [¶]Ohio State University Interdisciplinary Nutrition Program, and [‖]Center for RNA Biology, Ohio State University, Columbus, Ohio 43210

Edited by Ursula Jakob

Genome-wide analyses have revealed that during metal ion starvation, many cells undergo programmed changes in their transcriptome or proteome that lower the levels of abundant metalloproteins, conserving metal ions for more critical functions. Here we investigated how changes in cellular zinc status affect the expression and activity of the zinc-requiring Pho8 alkaline phosphatase from fission yeast (*Schizosaccharomyces pombe*). In *S. pombe*, Pho8 is a membrane-tethered and processed glycoprotein that resides in the vacuole. Using alkaline phosphatase activity assays along with various biochemical analyses, we found that Pho8 is active when zinc is plentiful and inactive when zinc is limited. Although Pho8 activity depended on zinc, we also found that higher levels of *pho8* mRNAs and Pho8 protein accumulate in zinc-deficient cells. To gain a better understanding of the inverse relationship between *pho8* mRNA levels and Pho8 activity, we examined the effects of zinc on the stability and processing of the Pho8 protein. We show that Pho8 is processed regardless of zinc status and that mature Pho8 accumulates under all conditions. We also noted that alkaline phosphatase activity is rapidly restored when zinc is resupplied to cells, even in the presence of the protein synthesis inhibitor cycloheximide. Our results suggest that *S. pombe* cells maintain inactive pools of Pho8 proteins under low-zinc conditions and that these pools facilitate rapid restoration of Pho8 activity when zinc ions become available.

Transition metals such as zinc, iron, and copper are required for the function of a wide range of proteins. As these metals can also be toxic when in excess, most organisms use a variety of mechanisms to control the acquisition, storage, distribution, utilization, and/or export of these essential metals to balance proteomic requirements for a specific metal ion with its availability (1–3).

One widely occurring mechanism to adapt to low levels of metal ions in the diet is a programmed sparing response to reduce the levels of abundant metalloproteins found within cells. These proteomic adaptations can result from changes at the transcriptional, posttranscriptional, or posttranslational level and are often accompanied by up-regulation of compensatory proteins or pathways that do not require a metal cofactor or that use an alternative metal cofactor (4–9). In addition to conserving and salvaging metal ions for essential functions, metal-sparing responses also facilitate the reallocation of metal ions in cells and prevent cells from synthesizing high levels of nonfunctional proteins, which, in the absence of the correct metal ion, are potentially more prone to misfolding or mismetalation (10, 11).

In this report, we used *Schizosaccharomyces pombe* as a model system to investigate how changes in cellular zinc status affect the activity of the vacuolar Pho8 alkaline phosphatase. We chose to study Pho8 as it belongs to a well-characterized family of proteins that bind multiple zinc ions (12). Additionally, in other yeasts, alkaline phosphatases are targeted for degradation under low-zinc conditions, suggesting that these proteins may be removed as part of a zinc-sparing or -salvaging response (13). We show that, in fission yeast, Pho8 activity depends on cellular zinc status and that it is only active when zinc ions are plentiful. Unexpectedly, we also found that higher levels of *pho8* transcripts and Pho8 protein accumulate in zinc-limited cells, whereas Pho8 activity depends on zinc. Although, at first, it seems surprising that cells would synthesize and process higher levels of an inactive enzyme under conditions of zinc deficiency, we also find that Pho8 is rapidly activated by readdition of zinc. We propose that increased expression of Pho8 under low-zinc conditions is a proactive mechanism to enable cells to rapidly restore Pho8 activity when zinc ions are available.

Results

Pho8 activity in fission yeast depends on zinc

Fission yeast express two enzymes with alkaline phosphatase activity: Pho8, a membrane-tethered vacuolar enzyme that is predicted to bind one magnesium ion and two zinc ions per monomer, and Pho2, an unrelated cytosolic enzyme of unknown function (14). To examine the effects of zinc on Pho2 and Pho8 function, we measured alkaline phosphatase activity in WT cells and in *pho2*Δ and *pho8*Δ mutants that were grown overnight in a zinc-limited minimal medium (ZL-EMM)[2] sup-

This work was supported by National Institutes of Health Grant RO1 GM105695 (to A. J. B.) and by the Office of the Director of the National Institutes of Health under Award S10OD023582. The authors declare that they have no conflicts of interest with the contents of this article. The content is solely the responsibility of the authors and does not necessarily represent the official views of the National Institutes of Health.

This article contains Figs. S1 and S2 and Table S1.

[1] To whom correspondence should be addressed: Dept. of Human Nutrition, Ohio State University, 1787 Neil Ave., Columbus, OH 43210. Tel.: 614-247-1559; Fax: 614-292-8880; E-mail: bird.96@osu.edu.

[2] The abbreviations used are: ZL-EMM, zinc-limited Edinburgh minimal medium; EGS, ethylene glycol bis(succinimidyl succinate); TNAP, tissue nonspecific alkaline phosphatase; CDF, cation diffusion facilitator.

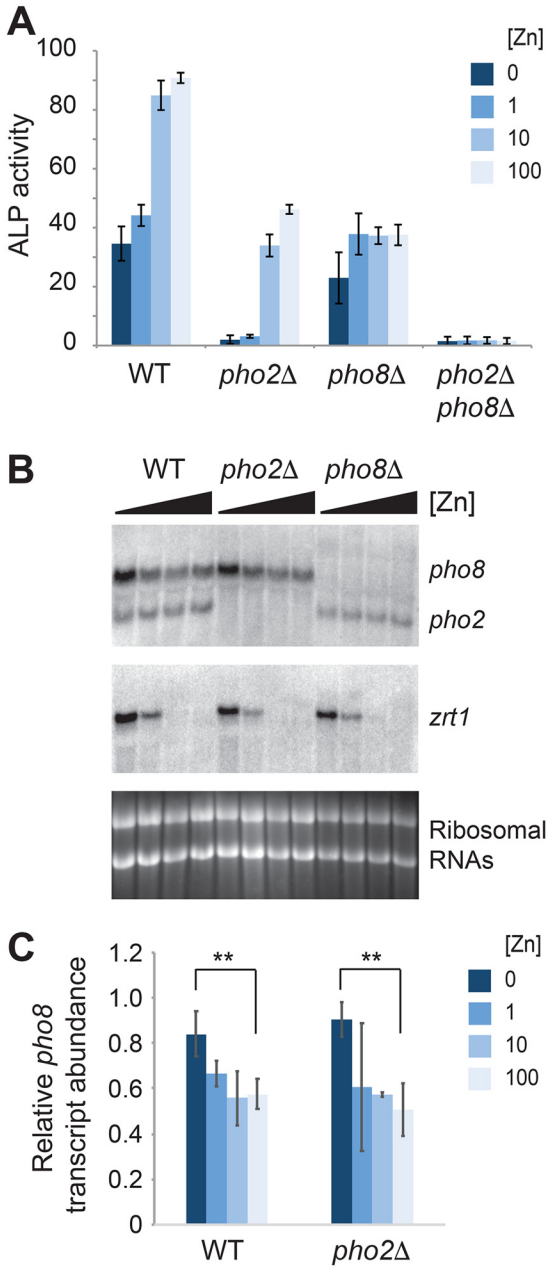

Figure 1. Effects of zinc on alkaline phosphatase activity and gene expression. *A*, WT, *pho2*Δ, *pho8*Δ, and *pho2*Δ *pho8*Δ cells were grown overnight in ZL-EMM supplemented with 0, 1, 10, or 100 μM zinc and assayed for alkaline phosphatase (*ALP*) activity. Activity is the mean of three independent repeats, with the *error bars* representing standard deviations. *B*, RNA blot analysis was performed using total RNA from WT, *pho2*Δ, and *pho8*Δ cells that were grown overnight in ZL-EMM supplemented with 0, 1, 10, or 100 μM zinc. RNA blots were probed for *pho8*, *pho2*, and *zrt1* mRNAs, with ribosomal RNAs shown as loading controls. *C*, relative levels of *pho8* transcripts normalized to ribosomal RNAs. Data are shown as the mean ± S.D. from three independent replicates. *p* values were determined using two-tailed unpaired Student's *t* test. **, $p < 0.01$.

plemented with 0–100 μM zinc. As shown in Fig. 1*A*, ~2-fold higher levels of alkaline phosphatase activity were detected in zinc-replete WT cells compared with zinc-limited cells. This activity depended on Pho2 and Pho8, as deletion of *pho2* and *pho8* nearly abolished alkaline phosphatase activity under all growth conditions, whereas deletion of *pho2* or *pho8* led to reduced but measurable alkaline phosphatase activity. We also found an ~10-fold increase in alkaline phosphatase activity in *pho2*Δ cells in the presence of 100 μM zinc, whereas in *pho8*Δ cells, alkaline phosphatase activity was detected under both zinc-limited and zinc-replete growth conditions. Taken together, these results indicate that Pho8 activity depends on zinc and that alkaline phosphatase activity in *S. pombe* is the sum of Pho8 and Pho2 activity.

The zinc-dependent changes in Pho8 activity are independent of changes in pho8 mRNA levels

The zinc-dependent increase in Pho8 activity could potentially result from changes in the levels of *pho8* mRNA and/or changes in the level, processing, or activity of the Pho8 protein. To determine whether *pho8* gene expression is affected by zinc status, RNA blot analysis was used to examine *pho8* transcript levels in cells grown over a range of zinc levels. RNA blots were also probed for *pho2* and *zrt1*, a gene that is specifically expressed when zinc is limited (15). In WT and *pho2*Δ cells, higher levels of *pho8* transcripts accumulated in zinc-limited cells compared with zinc-replete cells (Fig. 1, *B* and *C*), indicating that *pho8* is expressed at a higher level under conditions where the Pho8 protein is not active.

In *S. pombe*, a transcription factor called Loz1 plays a central role in zinc homeostasis by inhibiting gene expression when zinc is in excess (15, 16). To determine whether *pho8* expression depends on Loz1, we examined *pho8* transcript levels in WT and *loz1*Δ cells grown over a range of zinc levels. Deletion of *loz1* resulted in higher levels of *pho8* transcripts accumulating in zinc-replete cells, consistent with Loz1 facilitating repression of *pho8* gene expression under high-zinc conditions (Fig. 2*A*). To test whether these changes also affect the Pho8 protein level, we expressed the Pho8-GFP fusion protein from the *pho8* promoter. This fusion protein accumulated at higher levels in zinc-deficient cells in a manner that depended on Loz1 (Fig. 2*B*). Taken together, these results suggest that *pho8* is repressed in a Loz1-dependent manner when zinc is in excess and that growth under low-zinc conditions leads to derepression of *pho8* gene expression, which, in turn, leads to higher levels of *pho8* transcripts and Pho8 protein accumulation under this condition.

To further explore the effects of gene expression on alkaline phosphatase activity, we generated constructs to overexpress Pho8-GFP and Pho2-GFP fusion proteins from the strong constitutive phosphoglycerate kinase 1 (*pgk1*) promoter. Expression from the *pgk1* promoter was not affected by zinc (Fig. 3, *A* and *B*) and led to an ~16-fold increase in Pho8-GFP protein abundance under low-zinc conditions and an ~27-fold increase under high-zinc conditions relative to expression from the *pho8* promoter (Fig. 3*A*). Despite the large increase in Pho8-GFP abundance, Pho8 activity remained dependent on zinc, with growth in ZL-EMM + 100 μM Zn leading to an ~45-fold increase in alkaline phosphatase activity relative to the activity detected in cells grown with no added zinc (Fig. 3*C*). In contrast, overexpression of Pho2-GFP led to a large increase in alkaline phosphatase activity under all growth conditions (Fig. 3*D*). Taken together, these results indicate that the zinc-dependent changes in Pho8 activity are independent of changes in *pho8* gene expression and transcript levels.

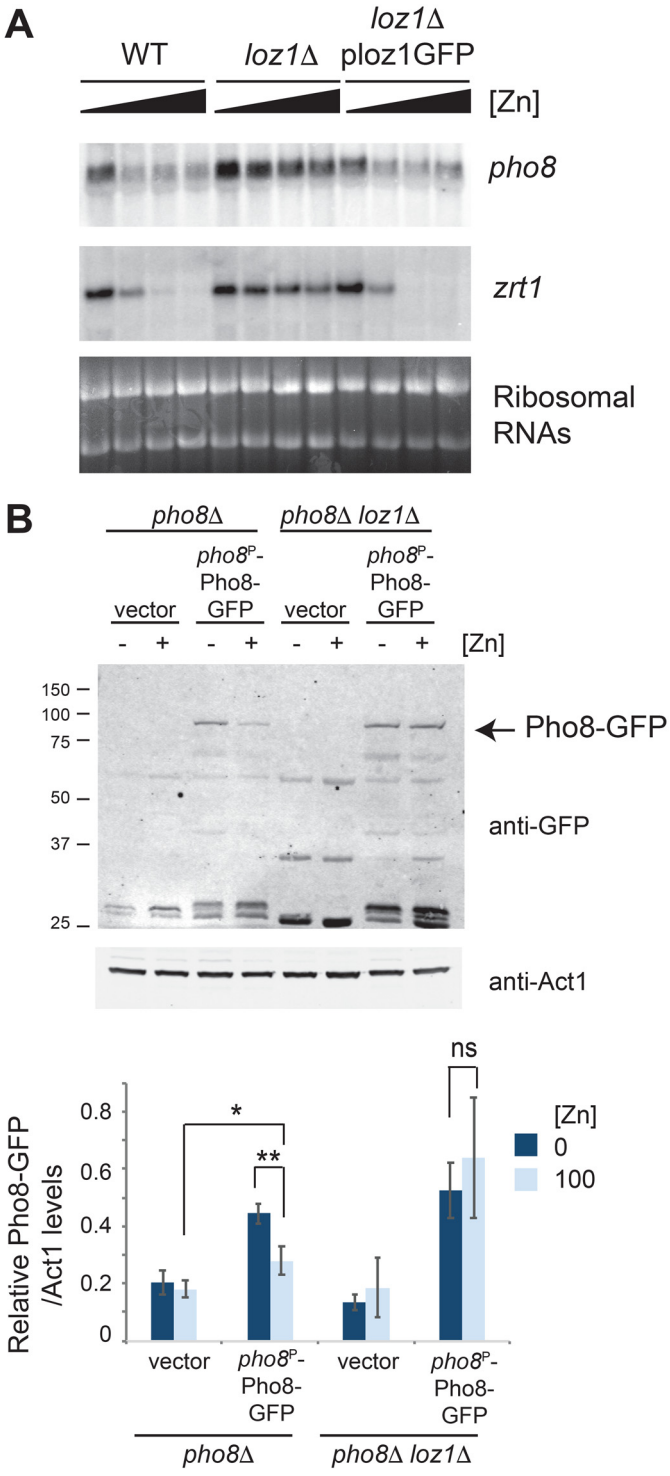

Figure 2. Pho8 is regulated in a manner that depends on Loz1. *A*, RNA blot analysis was performed using total RNA from WT, *loz1*Δ, and *loz1*Δ cells expressing a functional Loz1-GFP fusion protein. Cells were grown overnight in ZL-EMM supplemented with 0, 1, 10, or 100 μM zinc. RNA blots were probed for *pho8* and *zrt1* mRNAs. Ribosomal RNAs are shown as loading controls. *B*, immunoblot analysis of protein extracts prepared from *pho8*Δ and *pho8*Δ *loz1*Δ cells containing the empty vector or expressing Pho8-GFP from the *pho8* promoter. Cells were grown overnight in ZL-EMM supplemented with 0 or 100 μM zinc. The positions of the molecular mass markers in kilodaltons are shown on the *left*. *Bottom panel*, the mean ratio of Pho8-GFP/Act1 levels from three independent repeats, with *error bars* representing standard deviations. *p* values were determined using two-tailed unpaired Student's *t* test. *, $p < 0.05$; **, $p < 0.01$.

Processing of the Pho8 precursor is not affected by zinc status

Pho8 is synthesized as an inactive pro-form containing an inhibitory C-terminal propeptide (Fig. 4*A*), which, in fission yeast, is cleaved in a manner that depends on the vacuolar serine proteases Isp6 and Psp3 (17). Therefore, an alternative explanation for the zinc-dependent increase in Pho8 activity is that processing of the pro-form of Pho8 to the mature protein depends on the cellular zinc status. To examine Isp6- and Psp3-dependent processing, immunoblot analysis was used to compare the forms of Pho8-GFP that accumulated in WT and MGF317 cells. MGF317 is a quintuple deletion strain deficient in multiple proteases, including Isp6 and Psp3 (18). Incubation of immunoblots with GFP antibodies revealed two major bands in WT cells expressing Pho8-GFP (Fig. 4*B*). One of these bands was ~95 kDa in size and co-migrated with the inactive, unprocessed form of Pho8 that accumulated in MGF317 cells (Fig. 4, *B* and *C*). The other major band was ~27 kDa, which is the predicted size of the cleaved propeptide fused to GFP. Very low levels of this smaller band were detected in MGF317 cells, consistent with this latter designation.

When evaluating the effect of zinc status on the levels of the Pho8 precursor, we found that in some but not all experiments, lower levels of *pgk1*-driven Pho8-GFP precursor protein were detected in zinc-replete cells, suggesting that another factor potentially affected Pho8 protein abundance (Fig. 4*B*). As previous studies had shown that the activity of Isp6 increases as cells enter stationary phase (19) and that cells grown under zinc-limited conditions grow more slowly than cells grown under high-zinc conditions, we repeated the above experiments using cell lysates that were prepped from cells harvested at precise cell optical densities. Under both zinc-limited and zinc-replete conditions, Pho8-GFP processing depended on cell A_{600} (Fig. 4*D*). Despite the apparent differences in processing, Pho8 activity was only affected by zinc status (Fig. 4*E*). Based on these results, we conclude that, although processing of Pho8 depends on the growth phase of cells, zinc is the major factor that limits Pho8 activity *in vivo*.

The stability of Pho8 is not affected by zinc status

In the above experiments, we were unable to detect the mature form of Pho8 following processing. To visualize mature Pho8, we generated a new construct to express a *pgk1*-driven Pho8 protein containing an internal in-frame 3×HA epitope tag. The 3×HA tag was positioned so that it would remain fused to the C-terminal end of the mature Pho8 protein upon cleavage of the propeptide (Fig. 5*A*, *Pho8-HA*). We also generated a related strain expressing a truncated form of Pho8 that did not contain the 23-amino acid C-terminal inhibitory propeptide (Fig. 5*A*, *Pho8-HA* ΔC). Expression of the Pho8-HA and Pho8-HA ΔC fusion proteins in *pho2*Δ *pho8*Δ cells resulted in ~6.5-fold and ~5-fold increases in alkaline phosphatase activity under high-zinc conditions, respectively, compared with endogenous *pho8* under this condition, indicating that both constructs were functional (Fig. 5*B*, *pho2*Δ *vector*).

To determine whether zinc status affects the stability of the mature Pho8 protein, immunoblot analyses were performed using protein extracts prepared from *pho2*Δ *pho8*Δ and

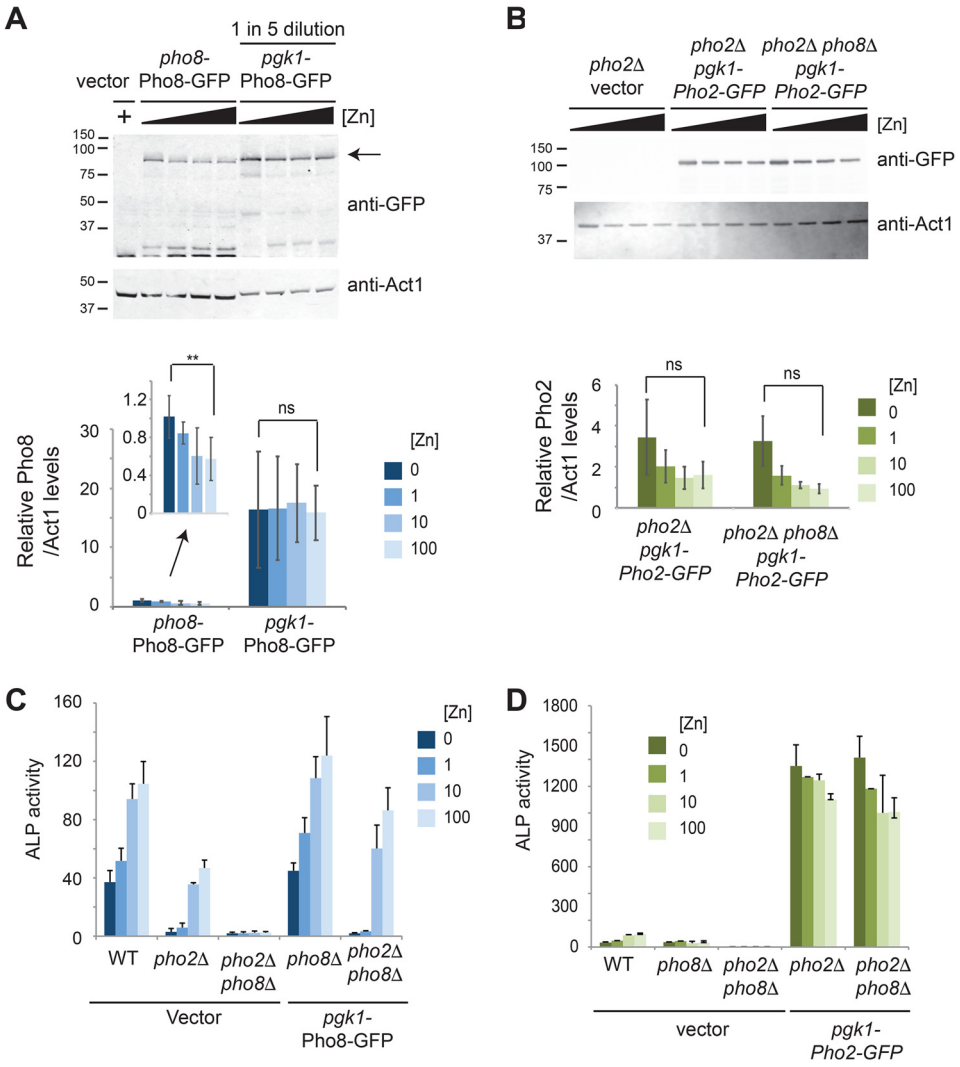

Figure 3. Effects of overexpression of *pho8* and *pho2* on alkaline phosphatase activity. *A*, immunoblot analysis of protein extracts prepared from *pho8*Δ cells expressing the indicated fusion proteins following growth in ZL-EMM supplemented with 0, 1, 10, or 100 μM zinc or the empty vector following growth in ZL-EMM and 100 μM zinc. Protein extracts prepared from *pho8*Δ cells expressing *pgk1*-Pho8-GFP were diluted 5-fold. The positions of the molecular mass markers in kilodaltons are shown on the *left*, and the *arrow* indicates the full-length Pho8-GFP protein. *Bottom panel*, the mean ratio of Pho8-GFP/Act1 levels from three independent repeats, with *error bars* representing standard deviations. **, $p < 0.01$; *ns*, not significant. *B*, immunoblot analysis was performed as described in *A* with the indicated strains. *C*, WT, *pho2*Δ, and *pho2*Δ *pho8*Δ cells bearing the empty vector and *pho8*Δ and *pho2*Δ *pho8*Δ cells expressing Pho8-GFP were assayed for alkaline phosphatase (*ALP*) activity following growth overnight in ZL-EMM supplemented with 0, 1, 10, or 100 μM zinc. Activity is the mean of three independent repeats, with the *error bars* representing standard deviations. *D*, WT, *pho2*Δ, and *pho2*Δ *pho8*Δ cells bearing the empty vector, and *pho2*Δ, and *pho2*Δ *pho8*Δ cells expressing Pho2-GFP were grown and assayed for alkaline phosphatase activity as described in *C*.

MGF317 cells expressing Pho8-HA or Pho8-HA ΔC. Two major bands were detected in *pho2*Δ *pho8*Δ cells expressing Pho8-HA (Fig. 5*C*). The larger band co-migrated with the unprocessed Pho8-HA protein detected in MGF317 cells, whereas the smaller band co-migrated with the mature Pho8-HA ΔC protein. These results are consistent with the larger Pho8-HA band being the unprocessed protein and the smaller band being the mature Pho8-HA protein.

When assessing the effects of zinc status on Pho8 protein levels, we found that the mature form of Pho8-HA and Pho8-HA ΔC proteins accumulated in both zinc-limited and zinc-replete cells (Fig. 5*C*). An unexpected result was that higher levels of the Pho8-HA ΔC protein were detected in zinc-limited cells, suggesting that the process of removing the inhibitory peptide leads to increased Pho8 turnover, particularly under low-zinc conditions. Although further studies are needed to test this hypothesis, these results further highlight that inactive forms of Pho8 accumulate in zinc-deficient cells. As a complementary approach to examine the effects of zinc binding on the stability of Pho8, we generated derivatives of Pho8-HA containing amino acid substitutions that prevented zinc from binding to the first zinc-binding site (Pho8-m1), the second zinc-binding site (Pho8-m2), or both sites (Pho8-m1/2). No alkaline phosphatase activity was detected in *pho2*Δ *pho8*Δ cells expressing these zinc-binding mutants, consistent with zinc binding to both sites being critical for function (Fig. 5*B*). When the effects of these mutations on Pho8 protein levels were analyzed by immunoblot analysis, slightly lower levels of the mature forms of Pho8-m1 and Pho8-m1/2 accumulated to lower levels in zinc-limited cells, whereas the levels of the mature Pho8-HA-m2 were not significantly altered by zinc levels (Fig. 5*D*). These results suggest that apo and holo forms of

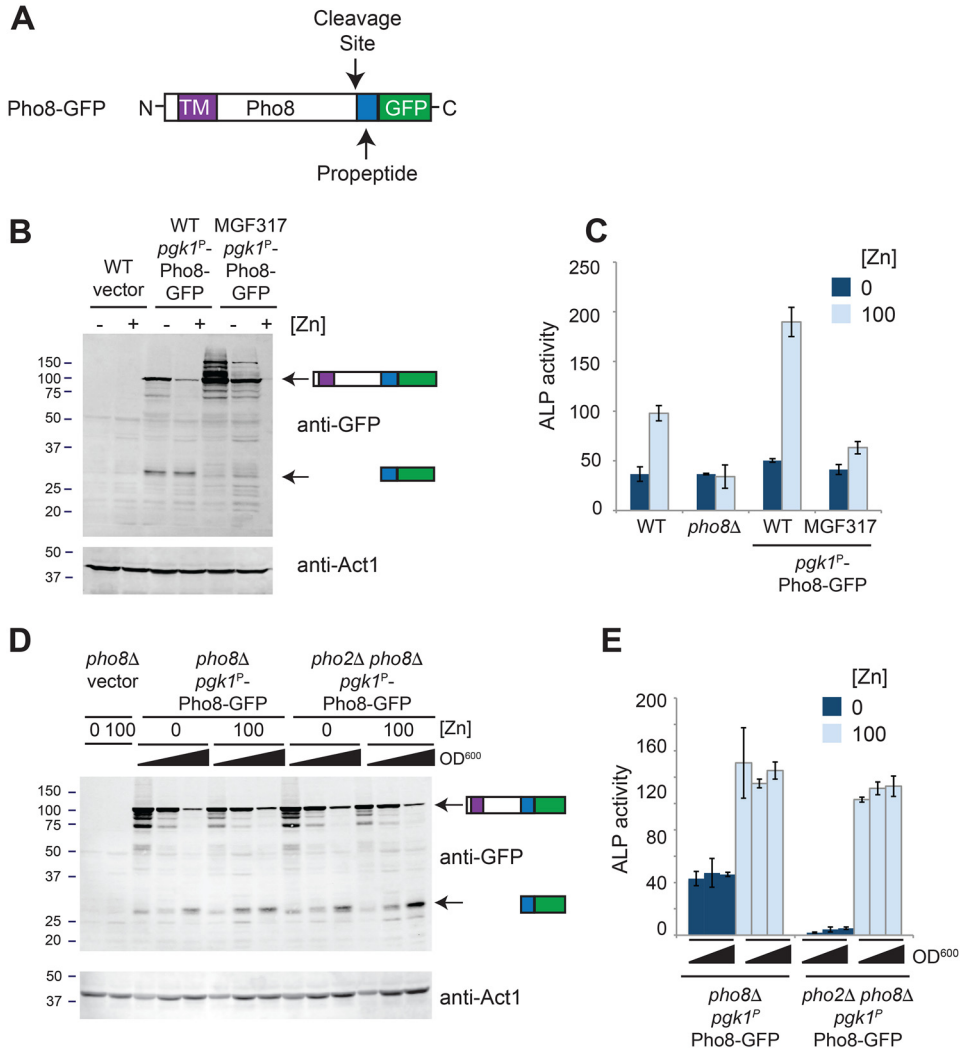

Figure 4. Processing of Pho8 depends on the growth phase and not zinc. *A*, schematic of Pho8-GFP, highlighting the positions of the transmembrane domain (*TM*), cleavage site, C-terminal propeptide, and GFP. *B*, WT cells bearing the empty vector and WT and MGF317 cells expressing Pho8-GFP were grown for 16 h overnight in ZL-EMM supplemented with 0 (−*Zn*) or 100 μM (+*Zn*) zinc, and protein extracts were prepared for immunoblot analysis. Immunoblots were incubated with anti-GFP antibodies and anti-Act1 antibodies as a loading control. The positions of the molecular mass markers in kilodaltons are shown on the *left*. *C*, alkaline phosphatase activity (*ALP*) was assayed in the indicated strains following growth for 16 h in ZL-EMM supplemented with 0 or 100 μM zinc. Each is the mean of three independent repeats, with the *error bars* representing standard deviations. *D* and *E*, *pho8*Δ and *pho2*Δ *pho8*Δ cells expressing Pho8-GFP were grown overnight in ZL-EMM supplemented with 0 or 100 μM zinc and harvested at an A_{600} of ~4.0, ~6.0, and ~8.0. Protein extract preparation and immunoblot analysis were performed as described above (*D*), or cell lysates were assayed for alkaline phosphatase activity as described above (*E*).

Pho8 accumulate in cells and that loss of zinc from site 1 may interfere with the processing or stability of the mature Pho8 protein under low-zinc conditions.

Pho8 dimerization is independent of zinc status

Both experimental and structural analyses of alkaline phosphatases from a wide range of species have shown that they exist and function as homodimers (12). Therefore, we next tested whether dimerization of Pho8 depends on zinc. To examine dimerization, whole-cell lysates were generated from zinc-limited and zinc-replete *pho2*Δ *pho8*Δ cells that co-expressed a *pho8*-driven Pho8-GFP fusion and a *pgk1*-driven Pho8-HA fusion. The lysates were then added to protein A magnetic beads that had been preincubated with anti-GFP antibodies. After incubation for 3 h to allow binding, the beads were washed, and proteins were eluted. To determine whether the Pho8-GFP and Pho8-HA proteins physically interacted, immunoblots of the protein extracts were incubated with anti-HA antibodies. As shown in Fig. 6*A*, Pho8-GFP and Pho8-HA proteins were detected in immunoprecipitates from zinc-limited and zinc-replete cells, consistent with the Pho8-GFP and Pho8-HA proteins forming dimers under all growth conditions.

As a complementary approach to examine dimerization, we employed an ethylene glycol bis(succinimidyl succinate) (EGS) cross-linking assay (20). In these experiments, EGS is added to protein extracts prepared from zinc-limited and zinc-replete cells, and the levels of cross-linked Pho8 dimers were examined by immunoblot analyses. As controls for these experiments, protein extracts were also prepared from cells expressing Pho8-HA containing the G475S and E478K substitutions. We examined the effects of these genetic mutations on Pho8 dimerization, as the equivalent substitutions (G456S and E459K, respectively) in the related human tissue nonspecific alkaline phosphatase (TNAP) are predicted to cause the rare

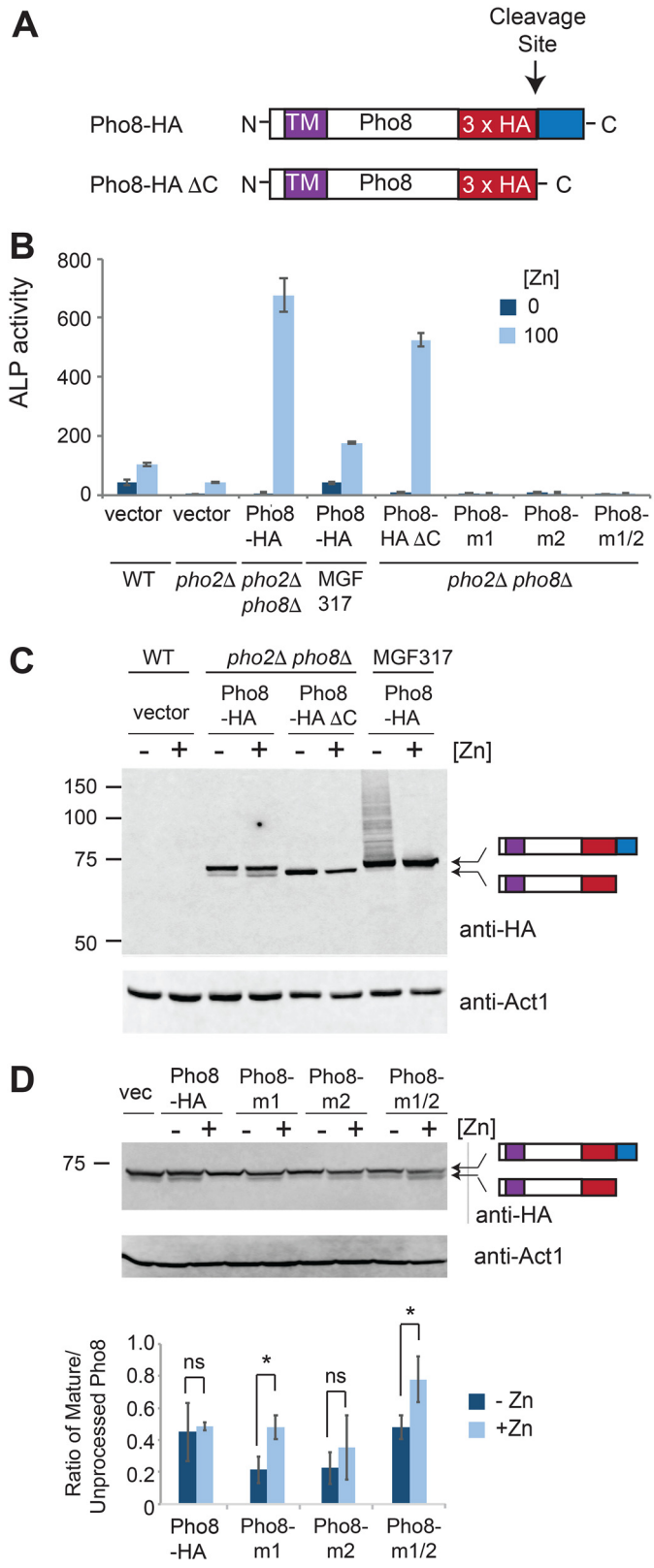

Figure 5. Pho8 stability is not affected by zinc status. *A*, schematic of Pho8-HA and Pho8-HA ΔC, highlighting the positions of the transmembrane domain (*TM*), 3×HA epitope, cleavage site, and C-terminal propeptide (*blue box*). *B*, alkaline phosphatase (*ALP*) activity was assayed in the indicated strains, which were grown in ZL-EMM supplemented with 0 or 100 μM zinc to an A_{600} of ~5. Activity is the mean of three independent repeats, with the *error bars* representing standard deviations. *C*, the indicated strains were grown in ZL-EMM supplemented with 0 or 100 μM zinc to an A_{600} of ~5, and protein extracts were prepared for immunoblot analysis. Immunoblots were incubated with anti-HA antibodies and anti-Act1 antibodies as a loading control. *D*, *pho8*Δ *pho2*Δ cells bearing the empty vector, Pho8-HA, or the indicated Pho8-HA zinc-binding mutants were grown overnight in ZL-EMM supplemented with 0 (−*Zn*) or 100 μM zinc (+*Zn*) to an A_{600} of ~5. Protein extract preparation and immunoblot analysis were performed as described above. *Bottom panel*, the mean ratio of mature to unprocessed Pho8-HA proteins from three independent repeats, with *error bars* representing standard deviations. *, $p < 0.05$; *ns*, not significant.

genetic disorder hypophosphatasia by impairing TNAP dimerization (21). Following addition of EGS to protein extracts, Pho8 dimers were detected under high- and low-zinc conditions in cells expressing Pho8-HA (Fig. 6, *B* and *C*). The introduction of mutations impairing dimerization (Pho8-HA G475S and Pho8-HA E478K) resulted in lower levels of Pho8 dimers and reduced Pho8 activity (Fig. 6, *B–D*). As addition of zinc did not decrease the levels of Pho8 dimers, we conclude that dimerization of Pho8 is not significantly altered by zinc status.

Activation of Pho8 by zinc

As zinc did not affect Pho8 stability, processing, or dimerization, we hypothesized that the activity of Pho8 is directly affected by cellular zinc status. In fission yeast, three CDF family members (Cis4, Zrg17, and Zhf1) transport zinc from the cytosol into the secretory pathway (22, 23). Cis4 and Zrg17 form a complex that transports zinc ions into the cis-Golgi, whereas Zhf1 plays a primary role in protecting the cytosol from zinc toxicity by transporting excess zinc ions into stores within the endoplasmic reticulum and, potentially, the vacuole (23, 24). To determine whether these transporters were required for the activation of Pho8, alkaline phosphatase activity was examined in *cis4* and *zrg17* deletion mutants that were grown overnight in ZL-EMM supplemented with 0–100 μM zinc (Fig. 7). As *zhf1*Δ cells are unable to grow in liquid medium supplemented with 10 μM zinc or more (22, 24), these cells were grown in ZL-EMM with 0 or 1 μM zinc. Deletion of *cis4* and/or *zrg17* did not significantly alter alkaline phosphatase activity. Unexpectedly, a slight increase in alkaline phosphatase activity was detected in *zhf1*Δ cells grown in ZL-EMM with 0 or 1 μM zinc.

To further assess the role of Zhf1 in zinc delivery to Pho8, we examined alkaline phosphatase activity following a zinc shock. In zinc shock experiments, cells are pregrown in zinc-deficient medium before being exposed to zinc (*i.e.* the zinc shock). As zinc-deficient cells express high levels of the Zrt1 zinc uptake system, this growth method results in a rapid influx of zinc immediately upon its addition to the growth medium (22). When a zinc shock was performed on zinc-limited WT cells, a rapid ~3-fold increase in alkaline phosphatase activity was detected (Fig. 8*A*, $t = 20$ min). This activity depended on Pho8, consistent with zinc entering the cells and being incorporated into Pho8, leading to its activation. Zinc shock also led to a rapid increase in alkaline phosphatase activity in *zhf1*Δ or *zrg17*Δ *cis4*Δ cells, indicating that zinc was incorporated into Pho8 in these mutants.

Potential explanations of the increase in alkaline phosphatase activity in the *zhf1*Δ and *zrg17*Δ *cis4*Δ strains following a zinc shock include that Zhf1 and the Cis4–Zrg17 complex have

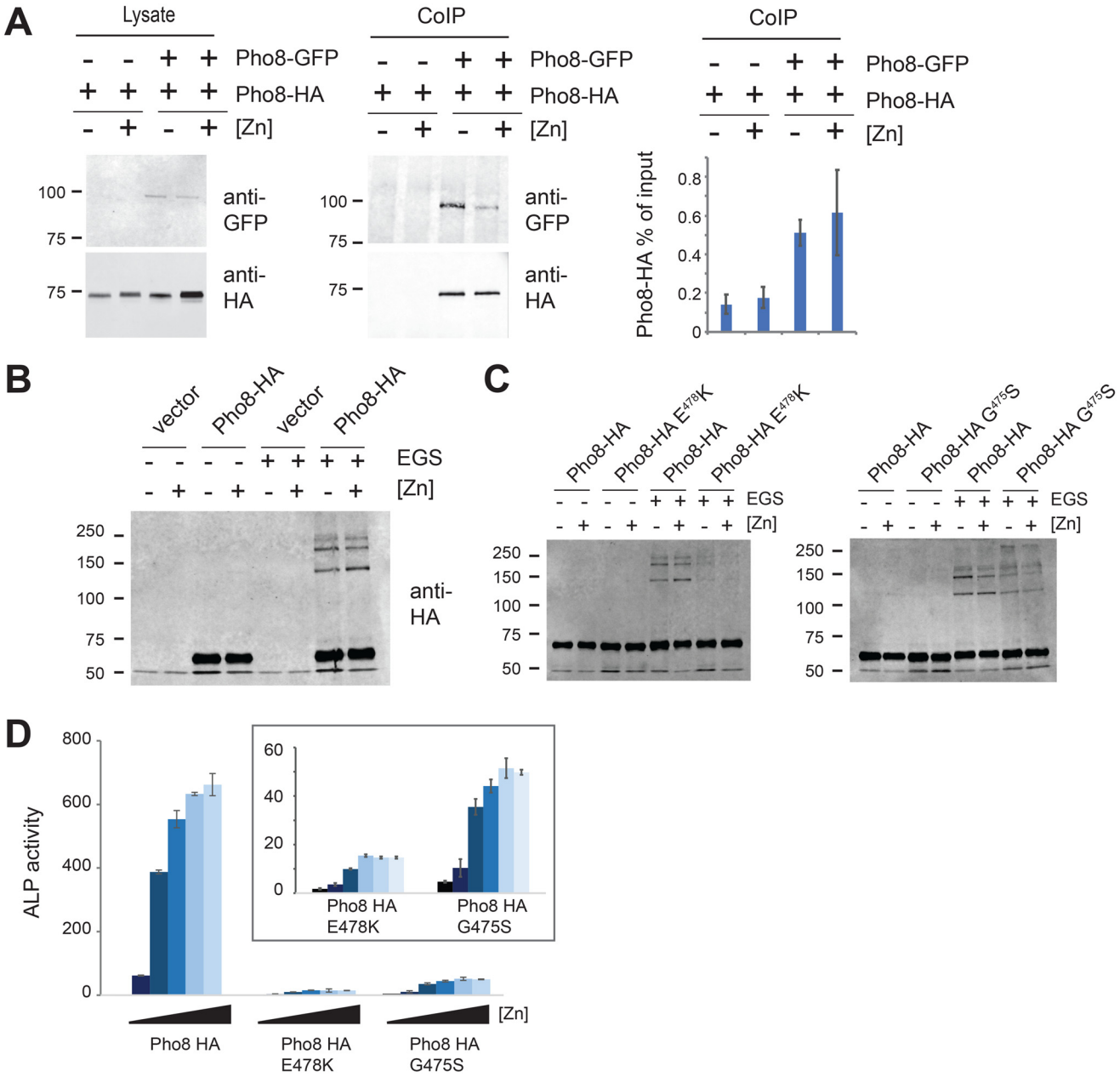

Figure 6. Dimerization of Pho8 is not dependent on zinc status. *A*, *pho2*Δ *pho8*Δ cells expressing *pgk1*-driven Pho8-HA or co-expressing *pho8*-driven Pho8-GFP and *pgk1*-driven Pho8-HA grown in ZL-EMM to an A_{600} of ~5. Cell lysates were incubated with anti-GFP-bound protein A beads and Pho8 co-immunoprecipitation (*CoIP*) complexes analyzed by immunoblotting. *Right panel*, the mean output signal for Pho8-HA relative to the input signal from three independent repeats, with *error bars* representing standard deviations. *B*, *pho2*Δ *pho8*Δ cells bearing an empty vector or Pho8-HA were grown in ZL-EMM to an A_{600} of ~5. Protein lysates from these cells were incubated with DMSO or EGS for 30 min, and Pho8 dimerization complexes were analyzed by immunoblotting. *C*, EGS cross-linking and immunoblotting were performed as described in *B*, using protein lysates prepared from *pho2*Δ *pho8*Δ cells bearing an empty vector, Pho8-HA, Pho8-HA E478K, or Pho8-HA G475S. *D*, alkaline phosphatase activity (*ALP*) was assayed in *pho2*Δ *pho8*Δ cells expressing Pho8-HA, Pho8-HA E478K, or Pho8-HA G475S, which were grown in ZL-EMM supplemented with 0, 1, 5, 10, 100, or 200 μM zinc to an A_{600} of ~5. The *inset* shows the results for Pho8 E478K and G475S mutants on an expanded scale. Activity is the mean of three independent repeats, with the *error bars* representing standard deviations.

a redundant role in supplying zinc ions and that there are other routes by which zinc ions enter the secretory pathway. To distinguish between these possibilities, we examined alkaline phosphatase activity in a *cis4*Δ *zrg17*Δ *zhf1*Δ triple mutant (Fig. 8*A*). In this strain, a significant decrease in alkaline phosphatase activity was detected following a zinc shock, suggesting that Zhf1 and the Cis4–Zrg17 complex have a largely redundant role in supplying zinc ions to Pho8.

To gain additional evidence that the Zhf1 and the Cis4–Zrg17 complex both supply zinc ions to Pho8, alkaline phosphatase activity was examined in WT cells and in various mutant strains expressing *pgk1*-driven Pho8-HA. In WT cells expressing this fusion, an ~18-fold increase in alkaline phosphatase activity was detected upon addition of zinc compared with those expressing the empty vector (Fig. 8*B*, $t = 0 + Zn$). A rapid increase in alkaline phosphatase activity was also observed in the *zrg17*Δ *cis4*Δ and *zhf1*Δ mutants but not in the triple mutant. Taken together, these results indicate that both Zhf1 and the Cis4–Zrg17 complex are able to supply zinc ions for Pho8 function.

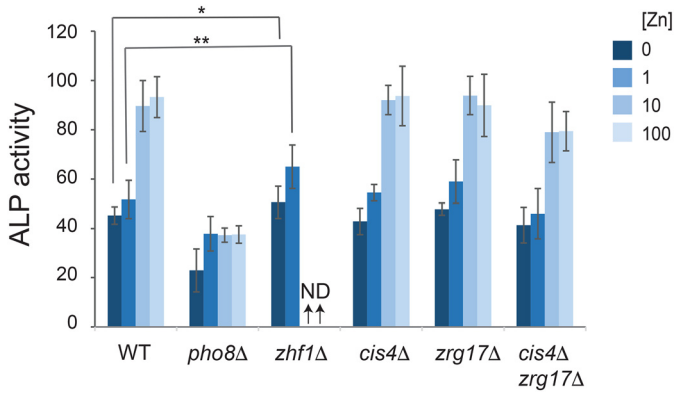

Figure 7. Alkaline phosphatase activity in CDF family mutants under steady-state growth conditions. Alkaline phosphatase (*ALP*) activity was assayed in the indicated strains, which were grown in ZL-EMM supplemented with 0, 1, 10, or 100 μM zinc to an A_{600} of ~5. Activity is the mean of three independent repeats, with the *error bars* representing standard deviations. **, $p < 0.01$; *, $p < 0.05$; *ND*, not determined.

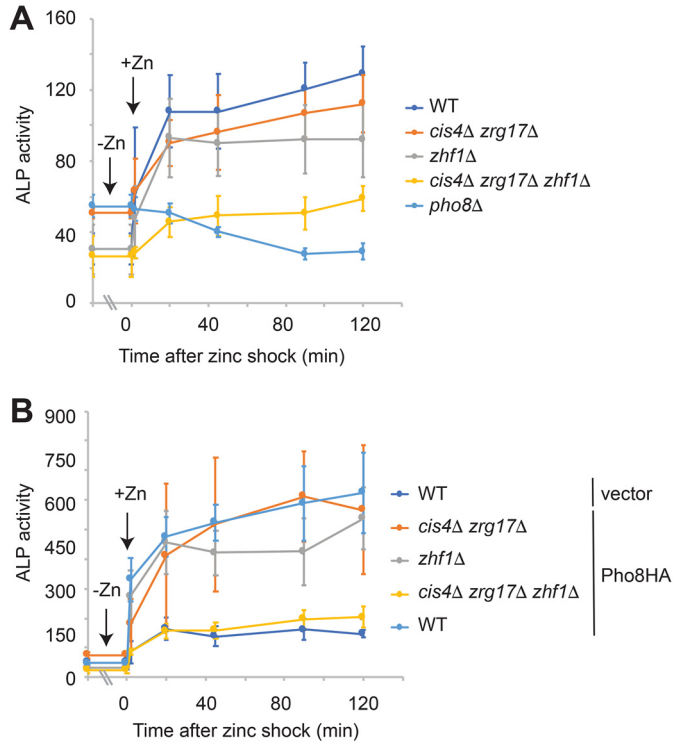

Figure 8. Zhf1 and the Cis4–Zrg17 complex have a redundant role in the activation of Pho8. *A*, the indicated strains were grown overnight in ZL-EMM to an A_{600} of ~5 ($t = -0$). Cells were then exposed to 100 μM zinc and harvested for alkaline phosphatase (*ALP*) activity assays at the indicated time points. Activity is the mean of three independent repeats, with the *error bars* representing standard deviations. *B*, the indicated strains expressing Pho8-HA or the empty vector were subject to zinc shock as described above, and alkaline phosphatase activity was assayed at the indicated time points. Activity is the mean of three independent repeats, with the *error bars* representing standard deviations.

If zinc is required for Pho8 activity, then why would cells express, process, and accumulate Pho8 under conditions of zinc deficiency? Most microorganisms are able to rapidly adapt to changes in the surrounding environment. Therefore, one potential explanation for cells maintaining an inactive pool of Pho8 is that as soon as zinc is available, it is incorporated into Pho8, allowing rapid restoration of activity. To test this hypothesis *pho2*Δ *pho8*Δ mutants expressing Pho8-HA ΔC from the *pgk1* promoter or Pho8-GFP from the *pho8* promoter were grown overnight in zinc-limited medium before being shocked with zinc. In contrast to the previous experiments, zinc-limited cells were also incubated for 30–120 min with the protein synthesis inhibitor cycloheximide prior to the zinc shock (Fig. 9*A* and Fig. S1). In fission yeast, the median half-life for a protein is ~12 h (25). Incubation with cycloheximide led to a large decrease in Pho8-HA ΔC and Pho8-GFP levels, suggesting that Pho8 has a shorter half-life than most proteins in *S. pombe* (Fig. 9*A*, *bottom panel*). Despite this decrease, zinc shock with 100 μM zinc led to an immediate increase in alkaline phosphatase activity, indicating that it is possible to activate Pho8 in the absence of new protein synthesis (Fig. 9, *A* and *B*, *top panels*). This increase was also dependent on Cis4, Zrg17, and Zhf1 (Fig. 9*C*). Taken together, these results are consistent with yeast maintaining an inactive pool of Pho8 under low-zinc conditions, which can be rapidly activated as soon as zinc is available.

Discussion

In this study, we investigated how changes in cellular zinc status affected the expression and activity of the fission yeast Pho8 vacuolar alkaline phosphatase. In general, increased expression of a gene in response to an environmental stress indicates that it has some important cellular function under this condition. Here we show that *pho8* mRNAs and Pho8 proteins accumulate at higher levels in zinc-deficient cells and that Pho8 is only active when zinc is in excess. Although it seems surprising for cells to express, synthesize, and process an inactive Pho8 protein under low-zinc conditions, we find a rapid increase in Pho8 activity when zinc is restored to cells. We propose that, under zinc-deficient conditions, fission yeast maintain an inactive pool of Pho8, which allows rapid activation and restoration of Pho8 activity as soon as zinc is available.

To gain a better understanding of why high levels of pho8 mRNA accumulate under low-zinc conditions, we examined *pho8* transcript abundance in a *loz1* deletion strain (Fig. 2). In fission yeast, the transcription factor Loz1 plays a primary role in controlling zinc homeostasis by regulating zinc acquisition and zinc sparing (15, 16, 26). When zinc levels are high, Loz1 is required for repression of gene expression, whereas, when zinc levels are low, Loz1 is inactive, leading to derepression of its target genes. Our results revealed higher levels of *pho8* mRNA in *loz1*Δ mutants under high-zinc conditions, consistent with *pho8* being repressed by Loz1.

In addition to alkaline phosphatases, multiple other enzymes reside or obtain their zinc cofactor within compartments of the secretory pathway, including protein disulfide isomerases and glycosylphosphatidylinositol-phosphoethanolamine transferases (27, 28). As some of these enzymes are essential for life, how would cells prioritize the transport of zinc to these proteins, and not to Pho8, when zinc is limited? One possibility is that mechanisms are present in *S. pombe* to deliver zinc ions to essential zinc proteins. For example, in humans, zinc-dependent activation of secreted TNAP depends on direct interaction with specific CDF zinc transporters (29). If related mechanisms were present in *S. pombe*, then, by prioritizing delivery of zinc ions to other proteins under low-zinc conditions, a situation

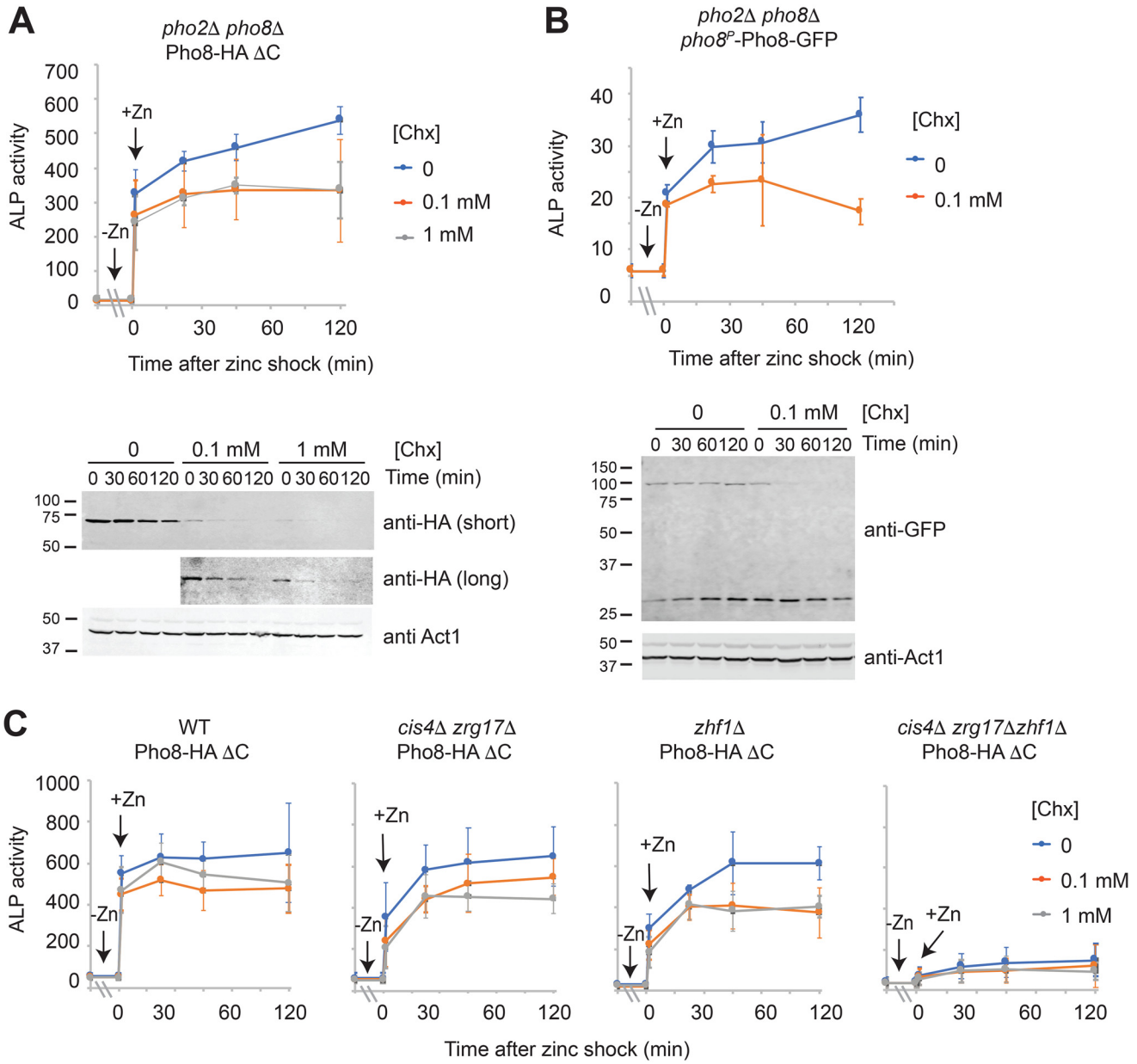

Figure 9. Activation of Pho8 by zinc. *A* and *B*, *pho2*Δ *pho8*Δ cells expressing *pgk1*-driven Pho8-HA ΔC (*A*) or *pho8*-driven Pho8-GFP (*B*) were grown overnight in ZL-EMM to an A_{600} of ~5. Cells were preincubated with 0, 0.1, or 1 mM cycloheximide for 2 h (*A*) or 30 min (*B*) before being exposed to 100 μM zinc ($t = 0$). Cells were then harvested for alkaline phosphatase (*ALP*) activity assays or immunoblot analysis at the indicated time points. Alkaline phosphatase activity and immunoblot analyses were performed as described in Fig. 3. *C*, the indicated strains expressing Pho8-HA ΔC were treated with cycloheximide for 2 h, shocked with 100 μM zinc, and assayed for alkaline phosphatase activity as described above.

may exist where there are insufficient zinc ions for metalation of Pho8.

An alternative possibility is that some aspect of Pho8 processing under conditions of zinc deficiency prevents it from binding its zinc cofactor or from being activated. A notable precedent for this type of control occurs in *Saccharomyces cerevisiae*. In this yeast, the Pho8 alkaline phosphatase is degraded in zinc-limited cells in a manner that depends on the Pep4 peptidase (13). Although Pho8 protein accumulates under low- and high-zinc conditions in *S. pombe*, we also detect multiple higher-molecular-weight species of Pho8 MGF317 cells. The strain MGF317 contains deletions in multiple genes, including the Psp3 and Isp6 vacuolar serine proteases, the carboxypeptidase Sxa2, the endonuclease Cdb4, and the putative di/aminopeptidase Xpa1, which is predicted to reside within the endoplasmic reticulum. At present, we do not know whether the higher-molecular-weight Pho8 species are linked to deletion of one or a combination of these genes. However, there are multiple mechanisms that could result in further post-translational modification of Pho8 in the secretory pathway. For example, misfolded proteins are substrates for endoplasmic reticulum–associated protein degradation, which leads to their ubiquitination and ultimate destruction by the proteasome (30). Recent studies in *S. cerevisiae* have also shown that Cot1, a vacuolar zinc transporter, is specifically ubiquitinated and targeted for degradation under low-zinc conditions (31). In other

current studies, we are investigating the nature of these modifications and whether they are linked to Pho8 inactivity under low-zinc conditions.

Our findings also include that multiple zinc transporters belonging to the CDF family have a largely redundant role in supplying zinc ions to Pho8. This differs from other characterized alkaline phosphatases that require zinc transport through specific zinc transporters for their activation. For example, in humans, activation of TNAP depends on zinc transport via ZnT5–ZnT6 heterodimers or ZnT7 homodimers (29). TNAP activation also depends on the presence of a diproline motif (PP) located in the second luminal loop of the ZnT5 and ZnT7 CDF family members (32). The zinc-dependent activation of Pho8 in *S. cerevisiae* is also dependent on zinc transport via the vacuolar Zrc1 and Cot1 transporters but not two other CDF family members (Msc2 and Zrg17) that transport zinc ions into the endoplasmic reticulum (13). As Zhf1 and Cot1 both contain the PP motif whereas Msc2 and Zrg17 do not, it has been suggested that the PP motif may also be important for the activation of alkaline phosphatases in yeast (32). Consistent with this hypothesis, the PP motif is conserved in Cis4 and Zhf1 in *S. pombe*. However, genetic mutations that disrupt this PP motif in Zhf1 have no effect on the zinc-dependent activation of Pho8 or Zhf1 transporter function (Fig. S2). Thus, our results indicate that the PP motif is not required for Pho8 activation in *S. pombe*, at least when zinc transport occurs via Zhf1.

In summary, our results show that Pho8 activity depends on cellular zinc status in *S. pombe*. As Pho8 activity is also dependent on zinc in *S. cerevisiae*, this regulation appears to be conserved in these evolutionarily distant yeasts. Despite this conservation, we find many differences in the regulation of Pho8 levels between the two yeast model systems. One of most striking differences is that, in *S. pombe*, *pho8* is expressed at higher levels under conditions of zinc deficiency, which leads to high levels of inactive Pho8 proteins accumulating in cells. Although many metalloenzymes are regulated at a transcriptional level by metalloregulatory factors, it is unusual for cells to increase the expression of the apo form of an enzyme when the metal cofactor is limited. In our work, we also show that addition of zinc to zinc-limited cells leads to rapid reactivation of Pho8, providing an explanation for why *S. pombe* up-regulates *pho8* expression under this condition. Although the presence of pools of apo or inactive forms of metalloenzymes in cells is well documented, it is not always possible to reactivate apo forms of protein by addition of the correct metal cofactor (34–36). Although we do not yet know why some apo-proteins are able to accumulate and be reactivated whereas others are not, it is noteworthy that deficiencies in metals such as zinc and iron are worldwide health problems, and many genetic diseases result from deficiencies in these and other metals ions (37–39). A greater understanding of the mechanisms by which apo-proteins are able to safely accumulate in cells and how some proteins can be repopulated with metals ions whereas others cannot will potentially provide more insight into the molecular and clinical consequences of metal ion deficiencies.

Experimental procedures

Yeast strains and growth conditions

The genotypes of yeast strains used in this study are shown in Table S1. Under nonselective conditions, strains were grown on yeast extract with supplements medium, which contained 0.5% yeast extract, 3% glucose, and 225 mg/liter adenine, uracil, and leucine. To select for the integration of plasmids, strains were grown in synthetic Edinburgh minimal medium (EMM), with the appropriate nutrient(s) being dropped out to allow for selection. To examine the effects of zinc status on alkaline phosphatase activity, cells were pregrown to exponential phase in yeast extract with supplements medium. Cells were then transferred to plastic tubes and washed twice in ZL-EMM, a derivative of EMM that does not contain zinc. Cells were inoculated into ZL-EMM with or without $ZnCl_2$ at an initial optical density of ~0.03 and were either grown overnight or to the indicated A_{600}.

Plasmids

The *pho8* gene was amplified from *S. pombe* genomic DNA by PCR and was cloned into the PstI/BamHI sites of the vector pBluescript SK (+) to generate pSK-pho8. The PstI/BamHI *pho8* fragment was then subcloned into similar sites in the vector JK-pgk1-GFP to generate Pho8-GFP. JK-pgk1-GFP contains 840 bp of the *pgk1* promoter inserted into the KpnI/EcoRI sites of the vector JK-GFP. A related strategy was used to generate Pho2-GFP, except that *pho2* was introduced as an EcoRI/BamHI fragment into JK-pgk1-GFP. The Pho8-HA construct was generated by an overlapping PCR using primers that introduced PstI and AscI sites at the 5′ and 3′ ends of the final overlap PCR product. Primers were designed so that the final overlap PCR product encoded the Pho8 protein containing three in-frame HA epitope tags inserted between amino acids 509 and 510 of Pho8. The PstI/AscI Pho8-HA fragment replaced the PstI/AscI pho8-GFP gene fusion in the plasmid Pho8-GFP to generate the plasmid Pho8-HA. A plasmid Pho8-HA ΔC was generated using PCR with Pho8-HA as a template. The PCR primers for this reaction were designed to introduce a stop codon immediately after the 3×HA coding region, which removes the last 23 amino acids of Pho8. To generate an additional pho8 vector that could be used for co-immunoprecipitation analysis, 406 bp of the *pho8* promoter were amplified using primers containing the KpnI/PstI restriction site. The KpnI/PstI-digested *pho8* promoter was then used to replace the KpnI/Pst1 *pgk1* promoter fragment in the vector Pho8-GFP. The *pho8* promoter and *pho8*-GFP gene fusion were then released by KpnI/SacI digestion and subcloned into similar sites in the vector JK210 (ATCC). For site-directed mutagenesis, the *pho8*-HA gene fusion was subcloned as a PstI/AscI fragment into the vector pSK-KanMX6, a derivative of pBluescript SK (+) containing an AscI site. QuikChange mutagenesis was then used to introduce mutations in the coding sequence of Pho8 that encoded amino acid substitutions preventing zinc binding to site 1 in Pho8 (D311A,H315A), to site 2 (D352A,H353A), or to both sites. The mutated products were subcloned into the vector JK-pgk1-GFP to create

Pho8-HA m1, Pho8-HA m2, and Pho8-HA m1/2, respectively. Correct clones were confirmed by DNA sequencing analysis.

Alkaline phosphatase activity assays

Alkaline phosphatase assays were performed as described previously (13), with the exceptions that 65 μl of 100 mM *p*-nitrophenyl phosphate was added to 650 μl of permeabilized cells to start the reaction, and the reaction was stopped by addition of 130 μl of 3 M NaOH. Units are calculated as 1000 $\times$ ΔA420/volume of cells assayed (in milliliters)/reaction time (in minutes)/A_{600} of the culture. Cell-free reactions were included as blanks. Activities shown represent the average values of three independent experiments. Where appropriate, data were analyzed by a Student's unpaired *t* test. $p < 0.05$ was considered statistically significant.

RNA extraction and RNA blotting

Total RNA was extracted using the hot acidic phenol method (40). For this method, 5 ml of cells was harvested by centrifugation at 3500 rpm for 2 min, and cell pellets were resuspended in 0.5 ml of Tris/EDTA/SDS buffer (10 mM Tris HCl (pH 7.5), 10 mM EDTA, and 0.5% SDS). Cell suspensions were lysed by addition of an equal volume of acid phenol and incubation for 1 h at 65 °C, with brief vortexing at 20-min intervals. Cell lysates were placed on ice for 2 min, followed by centrifugation at 12,000 rpm for 5 min. The upper aqueous layer was then transferred to a new tube, and total RNA was precipitated by addition of 3 volumes of ice-cold 100% EtOH. After centrifugation at 12,000 rpm for 10 min, total RNA was resuspended in 100–200 μl of 10 mM Tris (pH 8.5). Total RNA (10 μg) was analyzed by RNA blot hybridization as outlined by Sambrook and Russell (41). ^{32}P-labeled strand-specific RNA probes were generated using the MAXIscript T7 *in vitro* transcription kit (Thermo Fisher Scientific) according to the manufacturer's instructions. Signal intensities representing transcript abundance were visualized using GE Typhoon FLA 9500.

Protein extracts and immunoblotting

For experiments examining the processing and stability of Pho8-GFP and Pho8-HA fusions, protein lysates were prepared using a TCA precipitation (42). With this method, 5 ml of cells was harvested by centrifugation for 2 min at 3500 rpm. Cell pellets were resuspended in 0.5 ml of ice-cold buffer A (20 mM Tris (pH 8.0), 50 mM NH_4OAc, 0.5 mM EDTA, and 0.2 mM phenylmethylsulfonyl fluoride). Following addition of 0.5 ml of ice-cold TCA and ~0.3 g of glass beads, cells suspensions were lysed by vortexing three times for 30 s each, with 2 min on ice between each round of vortexing. Supernatants were transferred to a new tube, and proteins were pelleted by centrifugation for 10 min at 12,000 rpm. Pellets were resuspended in TCA sample buffer (3% SDS, 100 mM Tris base (pH 11), and 3 mM DTT) and boiled for 10 min. After removal of cell debris by centrifugation for 5 min at 12,000 rpm, protein extracts were separated on either 8%, 10%, or 12% (w/v) SDS-PAGE gels, followed by immunoblotting to a PVDF membrane. Immunoblots were incubated with anti-GFP (Millipore Sigma, G1544), anti-HA (12CA5, Millipore Sigma), and anti-Act1 (Abcam, ab3280; Nova Biochemicals, NB100-74340) primary antibodies and IR-Dye800CW and IRDye680 IgG (LICOR) secondary antibodies. Signal intensities were analyzed using the Odyssey IR imaging System (LICOR).

EGS cross-linking

Protein extracts for EGS cross-linking were generated using a method that was adapted from a procedure described previously (20). Briefly, 5 ml of yeast cells was harvested by centrifugation, washed once with cold distilled H_20, and transferred to 2-ml tubes. Cells were resuspended in 450 μl of HEGNT lysis buffer (20 mM HEPES (pH 7.5), 1 mM EDTA, 10% glycerol, 0.4 M NaCl, and 1% Triton X-100) containing a protease inhibitor mixture and 1 mM PMSF. Cells were lysed by vortexing with glass beads five times for 30 s each, with 2 mins on ice between pulses. After cell beads were removed by centrifugation, cell lysates were centrifuged for 10 min at 14,000 rpm. Cell lysates were transferred to a new microfuge tube, and total protein concentration was measured using a Bradford assay. For EGS cross-linking, 100 μg of protein extract was incubated with either DMSO or 1 mM EGS for 30 min at 24 °C. Reactions were quenched by addition of 50 mM glycine/0.025 mM Tris (pH 7.5).

Co-immunoprecipitation

25 ml of yeast cells was grown overnight in ZL-EMM supplemented with 0 or 100 μM zinc. Following centrifugation for 2 min at 3500 rpm, cells were washed twice in PBS before being resuspended in 1 ml of cold lysis buffer (20 mM Tris HCl (pH 8.0), 100 mM NaCl, 1% Triton-X100, and 2 mM EDTA) containing 1 mM PMSF. Cell suspensions were lysed by vortexing in the presence of zirconium beads five times for 1 min each, with 2 min on ice between pulses. Zirconium beads were removed by centrifugation for 1 min at 3500 rpm, and cell lysates were centrifuged at 14,000 rpm for 5 min. Cell lysates containing soluble proteins were transferred to a new microfuge tube, and total protein concentration was measured using a Bradford assay. For immunoprecipitation, 500 μg of cell lysates was incubated with protein A Dynabeads prebound with 2 μg of anti-GFP antibodies (Abcam, ab290) for 3 h at 4 °C. Dynabeads were washed three times in lysis buffer, and bound proteins were eluted by boiling in 50 μl of SDS-PAGE gel loading buffer (50 mM Tris-HCl (pH 6.8), 2% SDS, 0.1% bromphenol blue, and 100 mM DTT).

Author contributions—Y.-M. H. and A. J. B. conceptualization; Y.-M. H., D. M. B., H. C., S. W., and A. J. B. formal analysis; Y.-M. H., D. M. B., H. C., S. W., and A. J. B. investigation; Y.-M. H., D. M. B., H. C., and S. W. methodology; A. J. B. supervision; A. J. B. funding acquisition; A. J. B. writing-original draft; A. J. B. project administration.

Acknowledgments—We thank Dr. R. Michael Townsend and Andrew Weeks for critical reading of the manuscript and Dr. Kurt W. Runge for assistance with strain generation.

References

1. Chandrangsu, P., Rensing, C., and Helmann, J. D. (2017) Metal homeostasis and resistance in bacteria. *Nat. Rev. Microbiol.* **15,** 338–350 CrossRef Medline

2. Bird, A. J. (2015) Cellular sensing and transport of metal ions: implications in micronutrient homeostasis. *J. Nutr. Biochem.* **26,** 1103–1115 CrossRef Medline
3. Smith, A. D., Logeman, B. L., and Thiele, D. J. (2017) Copper acquisition and utilization in fungi. *Annu. Rev. Microbiol.* **71,** 597–623 CrossRef Medline
4. Gaballa, A., Antelmann, H., Aguilar, C., Khakh, S. K., Song, K. B., Smaldone, G. T., and Helmann, J. D. (2008) The *Bacillus subtilis* iron-sparing response is mediated by a Fur-regulated small RNA and three small, basic proteins. *Proc. Natl. Acad. Sci. U.S.A.* **105,** 11927–11932 CrossRef Medline
5. Ehrensberger, K. M., Mason, C., Corkins, M. E., Anderson, C., Dutrow, N., Cairns, B. R., Dalley, B., Milash, B., and Bird, A. J. (2013) Zinc-dependent regulation of the Adh1 antisense transcript in fission yeast. *J. Biol. Chem.* **288,** 759–769 CrossRef Medline
6. Martínez-Pastor, M., Vergara, S. V., Puig, S., and Thiele, D. J. (2013) Negative feedback regulation of the yeast CTH1 and CTH2 mRNA binding proteins is required for adaptation to iron deficiency and iron supplementation. *Mol. Cell. Biol.* **33,** 2178–2187 CrossRef Medline
7. Philpott, C. C., Leidgens, S., and Frey, A. G. (2012) Metabolic remodeling in iron-deficient fungi. *Biochim. Biophys. Acta* **1823,** 1509–1520 CrossRef Medline
8. Merchant, S., and Bogorad, L. (1987) Metal ion regulated gene expression: use of a plastocyanin-less mutant of *Chlamydomonas reinhardtii* to study the Cu(II)-dependent expression of cytochrome c-552. *EMBO J.* **6,** 2531–2535 CrossRef Medline
9. Kropat, J., Gallaher, S. D., Urzica, E. I., Nakamoto, S. S., Strenkert, D., Tottey, S., Mason, A. Z., and Merchant, S. S. (2015) Copper economy in *Chlamydomonas*: prioritized allocation and reallocation of copper to respiration vs. photosynthesis. *Proc. Natl. Acad. Sci. U.S.A.* **112,** 2644–2651 CrossRef Medline
10. Palm-Espling, M. E., Niemiec, M. S., and Wittung-Stafshede, P. (2012) Role of metal in folding and stability of copper proteins *in vitro*. *Biochim. Biophys. Acta* **1823,** 1594–1603 CrossRef Medline
11. MacDiarmid, C. W., Taggart, J., Kerdsomboon, K., Kubisiak, M., Panascharoen, S., Schelble, K., and Eide, D. J. (2013) Peroxiredoxin chaperone activity is critical for protein homeostasis in zinc-deficient yeast. *J. Biol. Chem.* **288,** 31313–31327 CrossRef Medline
12. Millán, J. L. (2006) Alkaline phosphatases: structure, substrate specificity and functional relatedness to other members of a large superfamily of enzymes. *Purinergic Signal.* **2,** 335–341 CrossRef Medline
13. Qiao, W., Ellis, C., Steffen, J., Wu, C. Y., and Eide, D. J. (2009) Zinc status and vacuolar zinc transporters control alkaline phosphatase accumulation and activity in *Saccharomyces cerevisiae*. *Mol. Microbiol.* **72,** 320–334 CrossRef Medline
14. Lock, A., Rutherford, K., Harris, M. A., Hayles, J., Oliver, S. G., Bähler, J., and Wood, V. (2019) PomBase 2018: user-driven reimplementation of the fission yeast database provides rapid and intuitive access to diverse, interconnected information. *Nucleic Acids Res.* **47,** D821–D827 Medline
15. Corkins, M. E., May, M., Ehrensberger, K. M., Hu, Y. M., Liu, Y. H., Bloor, S. D., Jenkins, B., Runge, K. W., and Bird, A. J. (2013) Zinc finger protein Loz1 is required for zinc-responsive regulation of gene expression in fission yeast. *Proc. Natl. Acad. Sci. U.S.A.* **110,** 15371–15376 CrossRef Medline
16. Ehrensberger, K. M., Corkins, M. E., Choi, S., and Bird, A. J. (2014) The double zinc finger domain and adjacent accessory domain from the transcription factor loss of zinc sensing 1 (loz1) are necessary for DNA binding and zinc sensing. *J. Biol. Chem.* **289,** 18087–18096 CrossRef Medline
17. Mukaiyama, H., Iwaki, T., Idiris, A., and Takegawa, K. (2011) Processing and maturation of carboxypeptidase Y and alkaline phosphatase in *Schizosaccharomyces pombe*. *Appl. Microbiol. Biotechnol.* **90,** 203–213 CrossRef Medline
18. Idiris, A., Tohda, H., Bi, K. W., Isoai, A., Kumagai, H., and Giga-Hama, Y. (2006) Enhanced productivity of protease-sensitive heterologous proteins by disruption of multiple protease genes in the fission yeast *Schizosaccharomyces pombe*. *Appl. Microbiol. Biotechnol.* **73,** 404–420 CrossRef Medline
19. Núñez, A., Dulude, D., Jbel, M., and Rokeach, L. A. (2015) Calnexin is essential for survival under nitrogen starvation and stationary phase in *Schizosaccharomyces pombe*. *PLoS ONE* **10,** e0121059 CrossRef Medline
20. Neef, D. W., Turski, M. L., and Thiele, D. J. (2010) Modulation of heat shock transcription factor 1 as a therapeutic target for small molecule intervention in neurodegenerative disease. *PLoS Biol.* **8,** e1000291 CrossRef Medline
21. Mornet, E., Stura, E., Lia-Baldini, A. S., Stigbrand, T., Ménez, A., and Le Du, M. H. (2001) Structural evidence for a functional role of human tissue nonspecific alkaline phosphatase in bone mineralization. *J. Biol. Chem.* **276,** 31171–31178 CrossRef Medline
22. Choi, S., Hu, Y. M., Corkins, M. E., Palmer, A. E., and Bird, A. J. (2018) Zinc transporters belonging to the cation diffusion facilitator (CDF) family have complementary roles in transporting zinc out of the cytosol. *PLoS Genet.* **14,** e1007262 CrossRef Medline
23. Fang, Y., Sugiura, R., Ma, Y., Yada-Matsushima, T., Umeno, H., and Kuno, T. (2008) Cation diffusion facilitator Cis4 is implicated in Golgi membrane trafficking via regulating zinc homeostasis in fission yeast. *Mol. Biol. Cell* **19,** 1295–1303 CrossRef Medline
24. Boch, A., Trampczynska, A., Simm, C., Taudte, N., Krämer, U., and Clemens, S. (2008) Loss of Zhf and the tightly regulated zinc-uptake system SpZrt1 in *Schizosaccharomyces pombe* reveals the delicacy of cellular zinc balance. *FEMS Yeast Res.* **8,** 883–896 CrossRef Medline
25. Christiano, R., Nagaraj, N., Fröhlich, F., and Walther, T. C. (2014) Global proteome turnover analyses of the yeasts *S. cerevisiae* and *S. pombe*. *Cell Rep.* **9,** 1959–1965 CrossRef Medline
26. Wilson, S., and Bird, A. J. (2016) Zinc sensing and regulation in yeast model systems. *Arch. Biochem. Biophys.* **611,** 30–36 CrossRef Medline
27. Solovyov, A., and Gilbert, H. F. (2004) Zinc-dependent dimerization of the folding catalyst, protein disulfide isomerase. *Protein Sci.* **13,** 1902–1907 CrossRef Medline
28. Mann, K. J., and Sevlever, D. (2001) 1,10-Phenanthroline inhibits glycosylphosphatidylinositol anchoring by preventing phosphoethanolamine addition to glycosylphosphatidylinositol anchor precursors. *Biochemistry* **40,** 1205–1213 CrossRef Medline
29. Fukunaka, A., Kurokawa, Y., Teranishi, F., Sekler, I., Oda, K., Ackland, M. L., Faundez, V., Hiromura, M., Masuda, S., Nagao, M., Enomoto, S., and Kambe, T. (2011) Tissue nonspecific alkaline phosphatase is activated via a two-step mechanism by zinc transport complexes in the early secretory pathway. *J. Biol. Chem.* **286,** 16363–16373 CrossRef Medline
30. Ruggiano, A., Foresti, O., and Carvalho, P. (2014) Quality control: ER-associated degradation: protein quality control and beyond. *J. Cell Biol.* **204,** 869–879 CrossRef Medline
31. Li, M., Koshi, T., and Emr, S. D. (2015) Membrane-anchored ubiquitin ligase complex is required for the turnover of lysosomal membrane proteins. *J. Cell Biol.* **211,** 639–652 CrossRef Medline
32. Fujimoto, S., Tsuji, T., Fujiwara, T., Takeda, T. A., Merriman, C., Fukunaka, A., Nishito, Y., Fu, D., Hoch, E., Sekler, I., Fukue, K., Miyamae, Y., Masuda, S., Nagao, M., and Kambe, T. (2016) The PP-motif in luminal loop 2 of ZnT transporters plays a pivotal role in TNAP activation. *Biochem. J.* **473,** 2611–2621 CrossRef Medline
33. Deleted in proof
34. Wang, Y., Weisenhorn, E., MacDiarmid, C. W., Andreini, C., Bucci, M., Taggart, J., Banci, L., Russell, J., Coon, J. J., and Eide, D. J. (2018) The cellular economy of the *Saccharomyces cerevisiae* zinc proteome. *Metallomics* **10,** 1755–1776 CrossRef Medline
35. Petrovic, N., Comi, A., and Ettinger, M. J. (1996) Identification of an apo-superoxide dismutase (Cu,Zn) pool in human lymphoblasts. *J. Biol. Chem.* **271,** 28331–28334 CrossRef Medline
36. Luk, E., Yang, M., Jensen, L. T., Bourbonnais, Y., and Culotta, V. C. (2005) Manganese activation of superoxide dismutase 2 in the mitochondria of *Saccharomyces cerevisiae*. *J. Biol. Chem.* **280,** 22715–22720 CrossRef Medline
37. Kambe, T., Tsuji, T., Hashimoto, A., and Itsumura, N. (2015) The physiological, biochemical, and molecular roles of zinc transporters in

zinc homeostasis and metabolism. *Physiol. Rev.* **95,** 749–784 CrossRef Medline
38. Gupta, A., and Lutsenko, S. (2009) Human copper transporters: mechanism, role in human diseases and therapeutic potential. *Future Med. Chem.* **1,** 1125–1142 CrossRef Medline
39. Camaschella, C. (2015) Iron-deficiency anemia. *N. Engl. J. Med.* **372,** 1832–1843 CrossRef Medline
40. Collart, M., and Oliviero, S. (1993) Preparation of yeast RNA. *Curr. Protoc. Mol. Biol.* **23,** 13.12.11–13.12.15 CrossRef
41. Sambrook, J., and Russell, D. W. (2000) Molecular Cloning: A Laboratory Manual, 3rd Ed., Cold Spring Harbor Laboratory Press, Cold Spring Harbor, NY
42. Peter, M., Gartner, A., Horecka, J., Ammerer, G., and Herskowitz, I. (1993) FAR1 links the signal transduction pathway to the cell cycle machinery in yeast. *Cell* **73,** 747–760 CrossRef Medline